A Review of Mobile Display Image Quality

Youn Jin Kim
(Digital Media & Communications R&D Center, Samsung Electronics Co. Ltd.)

Ⅰ. Introduction

Mobile devices such as smart phones and mobile phones are used in a diverse range of viewing conditions. We usually experience images on a mobile phone with a huge loss in contrast under bright outdoor viewing conditions; thus, viewing condition parameters such as surround effects, correlated colour temperature and ambient lighting have become of significant importance [1-2]. Recently, auxiliary attributes determining the mobile imaging were examined and the surround luminance and ambient illumination effects were considered as the first major factor[3]. Surround and ambient lighting effects on colour appearance modelling have been extensively studied to understand the nature of colour perception under various ambient illumination levels[4-7]; thus, this study intends to figure out characteristics of the human visual system(HVS) in spatial frequency domain by means of analysing the contrast discrimination ability of HVS.

It is to quantify the observed trend between surround luminance and contrast sensitivity and to propose an image quality evaluation method that is adaptive to both surround luminance and spatial frequency of a given stimulus. The non-linear behaviour of the HVS was taken into account by using contrast sensitivity function(CSF). This model can be defined as the square root integration of multiplication between display modulation transfer function(MTF) and CSF. It is assumed that image quality can be determined by considering the MTF of an imaging system and the CSF of human observers. The CSF term in the original SQRI model[8] is replaced by the surround adaptive CSF quantified in this study and it is divided by the Fourier transform of a given stimulus.

Ⅱ. Measuring and Modelling of the Surround Adaptive CSF

This study examined the effects of surround luminance on shape of spatial luminance CSF and reduction in brightness of uniform neutral patches shown on a computer controlled display screen is also assessed to explain the change of CSF shape. Consequently, a large amount of reduction in

contrast sensitivity at middle spatial frequencies can be observed; however, the reduction is relatively small for low spatial frequencies. In general, effect of surround luminance on the CSF appears the same to that of mean luminance. Reduced CSF responses result in less power of the filtered image; therefore, the stimulus should appear dimmer with a higher surround luminance.

1. Backgrounds

The CSF represents the amount of minimum contrast at each spatial frequency that is necessary for a visual system to distinguish a sinusoidal grating or Gabor patterns over a range of spatial frequencies from a uniform field. Physiologically, both parvocellular(P) and magnocellular(M) cells have receptive fields organised into two concentric antagonistic regions: a centre(on- or off-) and a surrounding region of opposite sense. This arrangement is common in vertebrates. The receptive fields of small bistratified cells appear to lack clear centre-surround organization[9]. The distributions of sensitivity within centre and surround mechanisms are usually represented by Gaussian profiles of a ganglion cell's receptive field. The spatial properties of the visual neurons are commonly inferred from a neuron's spatial modulation transfer function[10] or contrast sensitivity function[11] measured with grating patterns whose luminance is modulated sinusoidally. In practice, monochromatic patterns in which luminance varies sinusoidally in space are used. CSFs typically plot the reciprocal of the minimum contrast that is also referred to as threshold and provide a measure of the spatial properties of contrast-detecting elements in the visual system[12]. It is believed that CSF is in fact the envelope of the sensitivity functions for collections of neural channels that subserve the detection and discrimination of spatial patterns[13-14].

The first measurement of luminance CSF for the HVS was reported by Schade[15] in 1956 and the luminance CSF has been extensively studied over a variety of research fields - such as optics, physiology, psychology, vision and colour science - and the same basic trends were observed. Luminance CSF exhibits a peak in contrast sensitivity at moderate spatial frequencies(~ 5.0 cycles per degree; cpd)[12] and falls off at both lower and higher frequencies; thus, generally shows band-pass characteristics. The fall-off in contrast sensitivity at higher spatial frequency can be explained by spatial limitations in the retinal mosaic of cone receptors. The reduction in contrast sensitivity at lower spatial frequencies requires further neural explanations[16]. Centre-surround receptive fields are one possible reason for this low-frequency fall-off[17].

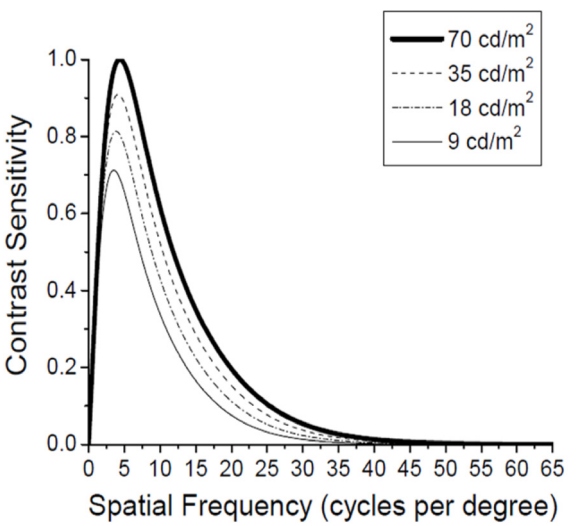

Fig. 1. Predicted CSF by Barten's model with various mean luminance levels for a field size of 5 degrees. As the mean luminance of the sinusoidal grating stimulus is decreased, contrast sensitivity at each spatial frequency decreases, and the maximum resolvable spatial frequency decreases as well. The peaks in the functions shift toward lower spatial frequencies and broaden.

CIE technical committee(TC) 1-60[18] has recently collected luminance CSF measurement data from various literatures[19-22]. Those data were measured using different experimental contexts; for instance, Campbell and Robson used Garbor patches and the others used sinusoidal gratings. The all data were normalised to unity at the maximum contrast sensitivity of each data set for a cross-comparison on a single plot. Consequently, they corresponded to one another and their trends are remarkably similar; therefore, they could be accurately fit by a single CSF model[22] in spite of the significant difference in conditions, methods and stimulus parameters.

The CSF model used was originally proposed by Barten as a function of spatial frequency and dependent on a field size(or viewing angle in degree) and mean luminance of the sinusoidal grating stimulus. As the mean luminance of the sinusoidal grating stimulus is decreased, the following variations occur(See Fig. 1). The contrast sensitivity at each spatial frequency decreases, and the maximum resolvable spatial frequency decreases. In addition, the shape of luminance CSF changes; the peaks in the functions shift toward lower frequencies, broaden, and eventually disappear[23-25].

The wealth of data in the literature also reports a variety of changes in CSF shape with senescence[26-30], eccentricity[31-35] and degree of adaptation to noise[36] in a given stimulus. Briefly, luminance CSFs for older subjects exhibit losses in contrast sensitivity at the higher frequencies, although much of the loss is attributed to optical factors[26, 37]. Sensitivity to the local contrast at the peripheral region can be measured by instructing the observer to fixate on a marker whilst the actual object is placed at some distance from the marker. The distance is usually expressed in an angular measure called ‘eccentricity’ and the contrast sensitivity is measured as a function of eccentricity. With increasing eccentricity, capillary coverage increases up to 40%[35]. Fairchild and Johnson[36] found the fact that the adapted luminance CSF relates to the reciprocal of the adapting stimulus’ spatial frequency. However, surround effects on the luminance CSF in spatial frequency domain appears to be less well investigated so far. Cox et al.[38] measured the effect of surround luminance on CSF and visual acuity using computer-generated sinusoidal gratings under a surround levels up to 90cd/m^2 for the purpose of ophthalmic practice in 1999. In consequence, reduced contrast sensitivity was measured under the highest surround luminance and the optimal surround level was found to be at 10 ~ 30% of mean luminance of a target stimulus. Precisely, contrast sensitivity increases when luminance of the surround increases from 0 to 10 ~ 20% of that of stimulus; however once the surround luminance exceeds the optimal level contrast sensitivity suddenly falls off.

Recently, portable display devices such as mobile phones and portable media players are viewed in a diverse range of surround luminance levels and we usually experience images on a mobile phone display with a huge loss in contrast under bright outdoor viewing conditions. Ambient illumination and surround have been thought of as the first major factor among the mobile environmental considerations[3]; therefore, it is worthy to measure the changes in luminance CSF shape under highly bright surrounds as a simulation of outdoor sunlight. In this article, luminance CSFs under different surround luminance levels measured in a previous study[39] are introduced and its applicability to image quality follows[40].

It should be noted that MTF of the display used is computed for each surround condition and divides the results from [39] in order to deduct the display's resolution term as well as effects of viewing flare. Because resolution of the display device used may limit the detectable contrast sensitivity of a human observer, the display factor should be discounted. In an equation form, let $F(u, v)$ represent MTF of a display which comes from the Fourier transformed line spread function(LSF). If the image from the display is filtered by CSF denoted by $H(u, v)$, the Fourier transform of the output $\psi(u, v)$ can be given by [8, 22]

$$\psi(u,v) = H(u,v)F(u,v), \quad (1)$$

where u and v are spatial frequency variables.

Therefore, CSF $H(u, v)$ can be estimated by deducting MTF $F(u, v)$ in linear system(See eq. (2)). Viewing flare is an additional luminance across the whole tonal levels from black to white and increases the zero frequency response only. More detailed discussions are followed in Results section.

$$H(u,v) = \psi(u,v)/F(u,v). \quad (2)$$

2. Contrast Sensitivity Adaptive to the Surround Luminance

(1) Compound Results of Contrast Threshold Perception and Physical Contrast

The compound results of contrast threshold perception and physical contrast loss are given in this section. They resulted from the increase of ambient illumination level causing both increase of surround luminance and viewing flare. Figure 2 depicts those ψ data for the three viewing conditions. Every data point was normalised to the

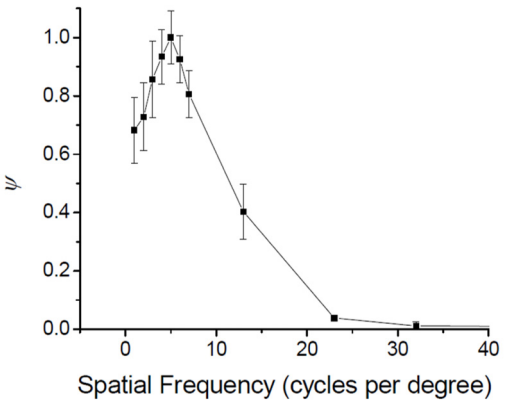

(a) Dark

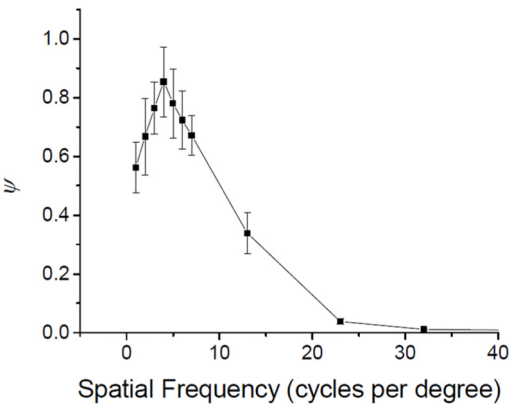

(b) Overcast

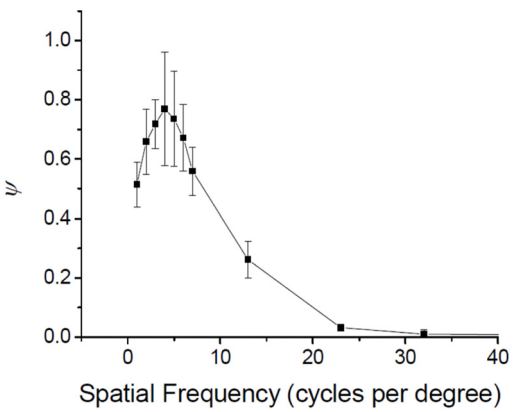

(c) Bright

Fig. 2. Measured data from[40] under 3 different ambient illumination conditions with linear interpolation for (a) dark (b) overcast and (c) bright. As the viewing condition changes from dark to overcast to bright, the data moved toward zero in general. The shape of the plots appears typical band-pass and the spatial frequency where the maximum contrast sensitivity occurred was moved toward a lower frequency.

unity at the maximum value obtained in dark(288) and adjacent data are linearly connected. Consequently, as the viewing condition changes from dark to overcast to bright, the data moved toward zero in general. The shape of the all three plots appears typical band-pass and the spatial frequency where the maximum contrast sensitivity occurred was moved toward a lower frequency, i.e. from 5 to 4 cpd. The compound effects of surround luminance and viewing flare on the contrast threshold perception and physical contrast loss seem to be similar to that of mean luminance as previously reported by the wealth of data in the literature as discussed in Introduction section. Error bars represent standard errors that can be defined as standard deviation divided by square root of number of observations.

(2) Deriving the Display MTF

It is often assumed that the point spread function(PSF) of a majority of commercial LCD monitors is a rectangle function, *rect*(*x*)[41-42], because the shape of a single pixel in LCDs is rectangular. Magnitude of the Fourier transform of the rectangle function can be expressed as a sinc function normalised by a factor of n.

$$MTF_i(u) = \alpha MTF_0(u) = \alpha|\mathrm{sinc}(\pi n\nu)|, \qquad (3)$$

where i represents the amount of viewing flare. For instance of this, MTF_0 shows the MTF for dark viewing condition so MTF_i is the MTF for a viewing condition where the amount of viewing flare is i cd/m^2.Theweighting factor α refers to the ratio of zero frequency response between $MTF_0(u)$ and $MTF_i(u)$ as given in Eq. (4). Practically, mean value of the PSF can be simply used instead of calculating zero frequency response of the MTF in Fourier domain therefore α values should be identical to the relative Michelson contrast to the dark viewing condition as can be expected(See Table 1).

The estimated MTF of the LCD monitor used in this study is presented in Fig. 3(See the solid line). Single-pixel size of the LCD is set to be 0.00474° in visual angle unit. The estimated MTFs for the higher illumination levels are shown in Fig. 3 as well represented by dashed and dotted lines.

$$\alpha = \frac{MTF_0(0)}{MTF_i(0)} = \frac{(L_{Max,0} - L_{Min,0})}{(L_{Max,i} - L_{Min,i})}. \qquad (4)$$

(3) Estimating CSF by Compensating for MTF

As given in eqs. (1) through 2 in Introduction section, CSFs for the three viewing conditions can

Table 1. The surround luminance function(φ)

	Dark	Overast	Bright
φ	1.000	0.534	0.191

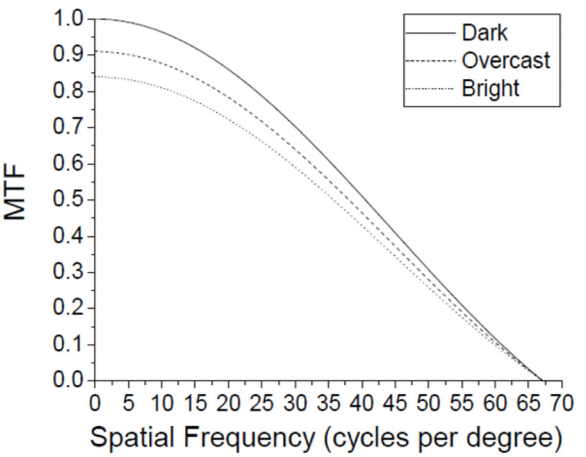

Fig. 3. MTF of the LCD used in this study and the approximated MTFs under two different levels of viewing flare. Single-pixel size of the LCD is set to be 0.00474° in visual angle unit. The compensation factors(α) for viewing flare for the three viewing conditions are listed in Table 1.

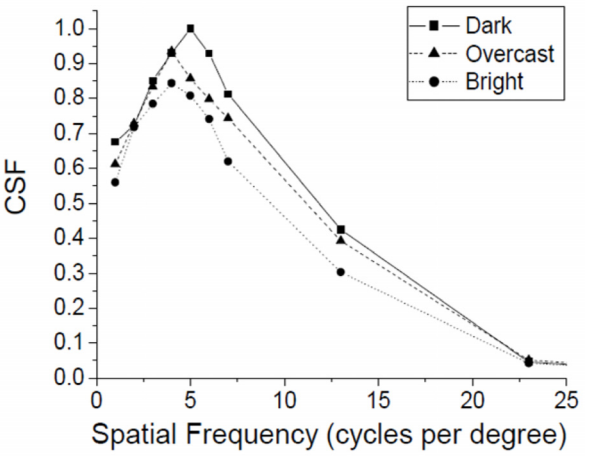

Fig. 4. Estimated CSF data points under 3 different surround luminance levels with linear interpolation. The all three plots show band-pass characteristics and the peak spatial frequency for dark is 5 cpd but moves to 4 cpd for overcast and bright. A large amount of reduction in contrast sensitivity at middle frequency area($4 < u < 13$) can be observed; however, little reduction in contrast sensitivity is found for lower frequencies($u < 4$).

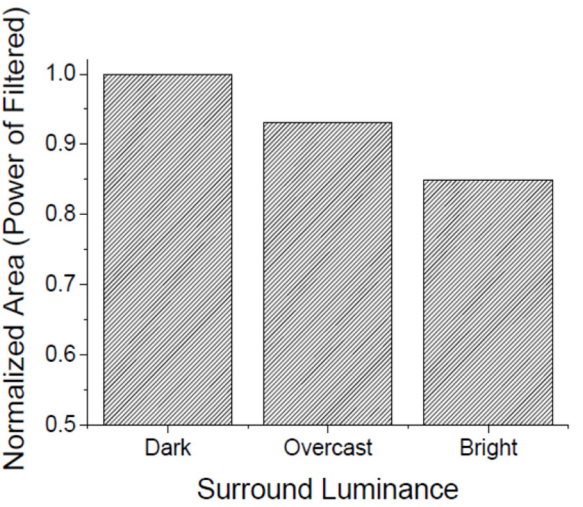

Fig. 5. Ratio of area of *psi* functions given in Figs. 4 (a) through (c). The area of a function or a filter correlates to the power of a filtered image. As can be seen, about 15 and 23% of the loss in power was occurred under overcast and bright, respectively due to the increase of ambient illumination.

be estimated by dividing ϕ by the corresponding MTFs as illustrated in Fig. 4. Data points for dark are linearly interpolated and represented by solid lines and dashed lines for overcast and dotted lines for bright. As can be seen, they show band-pass characteristics and the peak sensitivity for dark is observed at 5 cpd but it moves to 4 cpd for overcast and bright. The peak-shift appears more obvious compared to Fig. 2. However, it is not quite easy to yield significance of the shift on the sampling frequency of 1 cpd. A large amount of reduction in contrast sensitivity at middle frequency area($4 < u < 13$) can be observed; however, little reduction in contrast sensitivity is found for lower frequencies($u < 4$). Because the MTF converges to zero at near the maximum spatial frequency we sampled(68 cpd) so contrast sensitivity at 65 cpd is not investigated in the current section due to the limited display resolution.

Figure 5 illustrates the ratio of the area covered by the three linearly interpolated plots previously shown in Fig. 4. The area of a function or a filter correlates to the power of a filtered image. Area of each plot is normalised at the magnitude of the area for dark viewing condition. As can be seen, about 7 and 15% of the loss in power was occurred under overcast and bright, respectively due to the increase of surround luminance. The amount of power loss caused by the reduction in contrast sensitivity can be analogous to that of Michelson contrast reduction. As given in Table 1, Michelson contrast decrease reaches up to approximately 10 and 18% respectively for overcast and bright. It yields to the fact that the amount of physical contrast reduction is larger than that of power loss in CSF. In order to statistically verify the surround luminance and spatial frequency effects on the shape in CSF, two-way analysis of variance (ANOVA) was performed with surround luminance and spatial frequency as independent variables and contrast sensitivity as the dependent variable.

Significant effects could be found for both surround luminance and spatial frequency. Their P values were less than 0.0001. A value of $P<0.05$ was considered to be statistically significant in this study.

Generally, effect of surround luminance on the luminance CSF appears the same to that of mean luminance as previously discussed in Fig. 1. Because CSF response correlates to the filtered light in the ocular media, smaller CSF responses across the spatial frequency domain result in less power of the filtered image; thus, less amount of light can be perceived by the visual system. Therefore, the stimulus should appear darker under a higher surround luminance which can be verified through another set of experiments.

Ⅲ. Evaluating Image Quality

This section intends to quantify the effects of the surround luminance and noise of a given stimulus on the shape of spatial luminance CSF and to propose an adaptive image quality evaluation method. The proposed method extends a model called square-root integral(SQRI). The non-linear behaviour of the human visual system was taken into account by using CSF. This model can be defined as the square root integration of multiplication between display modulation transfer function and CSF. The CSF term in the original SQRI was replaced by the surround adaptive CSF quantified in this study and it is divided by the Fourier transform of a given stimulus for compensating for the noise adaptation.

1. Modeling the Effects of Surround Luminance

The surround luminance effects on CSF are quantified in this section. In order to compensate for the effects, a weighting function φ was multiplied to the adapting luminance that is denoted as L in [8]. Precisely, as previously mentioned in Background section, brightness of a stimulus can be affected by surround luminance increase so a function φ should be multiplied to L. For each surround, the following optimisation process was carried out.

Step 1. A CSF curve is predicted using Barten's model under a given surround condition. The adapting luminance can be obtained by measuring the mean luminance between black and white patches of the display.

Step 2. The predicted CSF curve is adjusted by changing the value of φ so that its maximum contrast sensitivity value can match that of the measured CSF data in [39] under the given surround condition. Note: in case the surround is dark, φ should equal to one.

Consequently, the maximum contrast sensitivity value of the adjusted CSF curve for overcast could match that of the measured CSF data points when φ equals to 0.534. In the case of bright, φ is found to be 0.339. Table 1 lists the obtained optimum φ values for the three surrounds along with their measured surround luminance levels. The relation between φ against the corresponding surround luminance(L_S) can be modelled by an exponential decay fit as given in eq. (5) and also illustrated in Fig. 12. Its exponential decaying shape appears similar to that of the image colour-quality model[43] that predicts the overall colour-quality of an image under various outdoor surround conditions. In addition, the change in "clearness," which is one of the psychophysical image quality attributes, caused by the illumination increase could also be modelled by an exponential decay function as well[44].

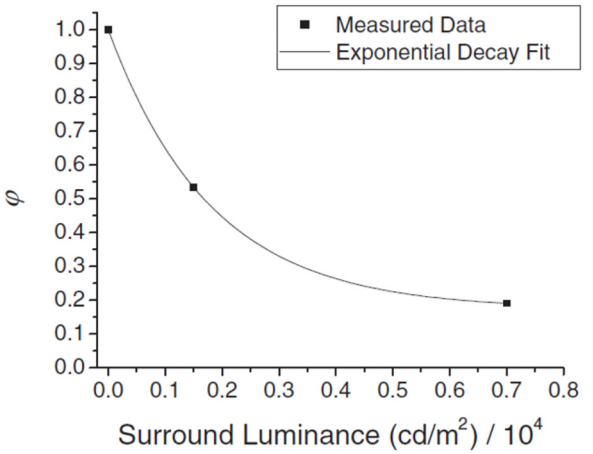

Fig. 6. Relation between the surround luminance factor (φ) and the normalised surround luminance($L_S/10^4$)

$$\phi = 0.17 + 0.83e^{-10^{-4}L_S/0.18}. \quad (5)$$

2. Adaptive SQRI

The adaptive SQRI ($SQRI_a$) can be expressed as eq. (6). The $M_t(u)$ in the original SQRI[22] is replaced by $M_{ta}(u)$ which represents the inverse of the adaptive CSF denoted as $CSF_a(u)$.

$$SQRI_a = \frac{1}{\ln 2}\int_0^{u_{\max}} \sqrt{\frac{MTF(u)}{M_{ta}(u)}}\frac{du}{u}, \quad (6)$$

where u denotes the spatial frequency and $1/M_{ta}(u)$ is

$$\frac{1}{M_{ta}(u)} = CSF_a(u) = \frac{au \times e^{(-bu)\sqrt{(1+c\times e^{bu})}}}{k \times img(u) + 1}.$$

The numerator of CSF_a shows the surround luminance adaptive CSF; a, b, and c are

$$a = \frac{540\times(1+0.7/\phi L)^{-0.2}}{1+\frac{12}{w(2+u/3)^2}},$$

$$b = 0.3(1+100/\phi L)^{0.15}, \text{and}$$

$$c = 0.06$$

where the adapting luminance L is the mean luminance between white and black on the display under a given surround luminance and φ is a weighting function for the surround luminance effect as previously given in eq. (5).

As[36] found the reciprocal relation between the adapted contrast sensitivity of the HVS and the adapting stimulus' spatial frequency, CSF_a is divided by Fourier transform of the given image. The denominator of the CSF_a shows amplitude of the Fourier transformed image information, $img(u)$. A constant k is multiplied to the magnitude of img(u) for normalisation as

$$k = 10^4 \times \frac{1}{\max(|img(u)|)}. \quad (7)$$

Since the denominator of $SQRI_a$ is Fourier transform of a given image, the model prediction can be proportional to the inverse of the image's spatial frequency. In order to attenuate any unwanted spatial frequency dependency of the image, the model prediction should be normalised by that of a certain degraded image expressed as

$$nSQRI_a = \frac{SQRI_a(Original)}{SQRI_a(^\circ raded)}, \quad (8)$$

where $nSQRI_a$ denotes a normalised $SQRI_a$ prediction and $SQRI_a(Original)$ and $SQRI_a(Degraded)$ respectively represent $SQRI_a$ predictions for a given original image and its degraded version.

The degraded image can be defined as an image of which its pixel resolution is manipulated to a considerably lower level, i.e., 80 pixels per inc. (ppi), while the original resolution was 200ppi., and luminance of each pixel is reduced to 25% of its original. The normalisation method makes $SQRI_a$ to predict the quality score of a given image

regardless the level of adapting spatial frequency. Since the overall dynamic range of $nSQRI_a$ in eq. (8) may be changed due to the normalisation process, it was re-scaled to a 9-category subjective scale[42] using a least-square method for each surround luminance condition. The rescaling process can be written as

$$J' = pJ + q, \tag{9}$$

where J' represents a re-scaled 9-category value of J, i.e., $nSQRI_a$ of an image. The scaling factors are denoted as p (slope) and q (offset) and the optimum scaling factors can be determined through a set of psychophysical experimental data from[40].

Scaling factors in eq. (9) optimised for the three viewing conditions are listed in Table 2. Magnitude of them is systematically changed from dark to overcast to bright and could be modelled by an exponential decay fitting of surround luminance L_S (see eqs. (10) and (11)). The predicted curves are compared with the computed scaling factors.

$$p = 1.16 + 2.36e^{-10^{-4}L_S/0.35}, \tag{10}$$

$$q = 0.35 - 5.38e^{-10^{-4}L_S/0.29}. \tag{11}$$

In Fig 7, the abscissa shows $nSQRI_a$ prediction values, which are re-scaled by the scaling factors listed in Table 2, and the ordinate shows the corresponding MOS.(Note that a 45° line is given for illustrating the data spread.) Different shaped

Table 2. Scaling factors for the viewing conditions

	Dark	Overast	Bright
Slope	3.93	2.69	1.47
Offset	-6.71	-2.89	-0.11

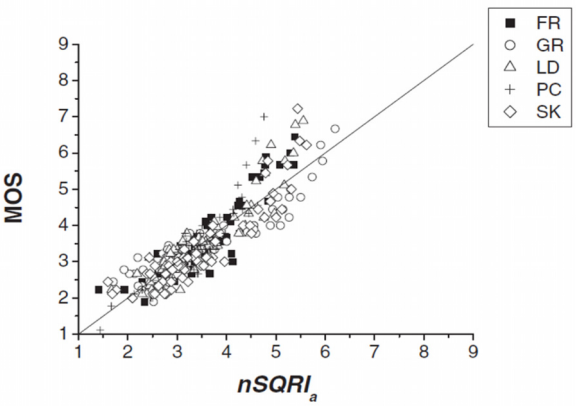

Fig. 7. Comparison between *nSQRIa* and their corresponding MOS across the three surrounds.

symbols represent different test images. For instance, the filled squares are for “Fruits(FR)”, circles for “Grass(GR)”, triangles for “Ladies(LD)”, crosses for “Picnic(PC)” and diamonds for “Skytower(SK)”. The model accuracy for the overall data sets can also be predicted by calculating a CV value[2, 6-7, 40, 44] between the two axes and it was 15 which is smaller than the mean observer accuracy (29) across the three surround conditions. Specifically, the CV between the two data sets was 18 for dark, 13 for overcast and 9 for bright and all are less than the corresponding mean observer accuracy. Note that the mean observer accuracy was 26 for dark, 32 for overcast and 30 for bright. Consequently, no significant image dependency of the model prediction was observed due to the spatial frequency normalisation procedure.

Ⅳ. Summary

The current research intends to quantify the surround luminance effects on the shape of spatial luminance CSF and to propose an image quality evaluation method that is adaptive to both surround luminance and spatial frequency of a given stimulus. The proposed image quality

method extends to a model called SQRI[8]. The non-linear behaviour of the HVS was taken into account by using CSF. This model can be defined as the square root integration of multiplication between display MTF and CSF. It is assumed that image quality can be determined by considering the MTF of the imaging system and the CSF of human observers. The CSF term in the original SQRI model was replaced by the surround adaptive CSF quantified in this study and it is divided by the Fourier transform of a given stimulus.

A few limitations of the current work should be addressed and revised in the future study. First, more accurate model predictions can be achievable when the actual display MTF is measured and used instead of the approximation. Then, a further improvement to the model prediction accuracy can be made when chromatic adaptation of the HVS is taken into account[45-46].

Reference

[1] N. Katoh, K. Nakabayashi, M. Ito, and S. Ohno, *J. Electron. Imag.,* **7**, 794 (1998).
[2] N. Mornoney, M. D. Fairchild, R. W. G. Hunt, C. Li, M. R. Luo, and T. Newman, *Proc. IS&T/SID Col. Imag. Conf.* (2002).
[3] Z. Li, A. K. Bhomik, and P. J. Bos (Wiley, 2008).
[4] C. Liu & M. D. Fairchild, *Proc.IS&T/SID Col. Img. Conf.* (2004).
[5] C. Liu & M. D. Fairchild, *Proc.IS&T/SID Col. Img. Conf.* (2007).
[6] S. Y. Choi, M. R. Luo and M. R. Pointer, *IS&T/SID Proc. Col. Img. Conf.* (2007).
[7] Y. Park, C. Li, M. R. Luo, Y. Kwak, D. Park, C. Kim, *IS&T/SID Proc. Col. Img. Conf.* (2007).
[8] P. G. Barten, *J. Opt. Soc. Am*, **7**, 2024 (1990).
[9] D. M. Dacey and B. B. Lee, *Nature*, **367**, 731 (1994).
[10] F. L. van Nes and M. A. Bouman, *J. Opt. Soc. Am.*, **57**, 401 (1967).
[11] C. Enroth-Cugell and J. G. Robson, *J. Physiol.*, **187**, 517 (1966).
[12] F. W. Campbell and J. G. Robson, *J. Physiol.*, **197**, 551 (1968).
[13] O. Braddick, F. W. Campbell, *J. Atkinson* (Springer-Verlag, 1978).
[14] N. Graham (Erlbaum, 1980).
[15] O. H. Schade, *J. Opt. Soc. Am.*, **46**, 721 (1956).
[16] S. Westland, H. Owens, V. Cheung, and I. Paterson-Stephens, *Col. Res. Appl.*, **31**, 315 (2006).
[17] B. A. Wandell (Sinauer Associates, 1995).
[18] E. Martinez-Uriegas (CIE, 2006).
[19] F. W. Campbell and J. G. Robson, *J. Physiol.*, **197**, 551 (1968).
[20] A. B. Watson, *Opt. Exp.*, **6**, 12 (2000).
[21] E. Martinez-Uriegas, J. O. Larimer, J. Lubin, and J. Gille (CIE, 1995).
[22] P. G. J. Barten (SPIE, 1999).
[23] A. M. Rohaly and G. Buchsbaum, *J. Opt. Soc. Am. A*, **6**, 312 (1989).
[24] A. S. Patel, *J. Opt. Soc. Am.* **56**, 689 (1966).
[25] R. L. de Valois, H. Morgan, and D. M. Snodderly, *Vision Res.*, **14**, 75 (1974).
[26] C. Owsley, H. Sekuler, and D. Siemsen, *Vision Res.*, **23**, 689 (1983).
[27] U. Tulunay-Keesey, J. N. ver Hoever, and C. Terkla-McGrane, *J. Opt. Soc. Am. A*, **5**, 2191 (1988).
[28] K. E. Higgins, M. J. Jaffe, R. C. Caruso, and F. deMonasterio, *J. Opt. Soc. Am. A*, **5**, 2137 (1988).
[29] A. M. Rohaly and C. Owsley, *J. Opt. Soc. Am. A,* **10**, 1591 (1993).
[30] S. Pardhan, *J. Opt. Soc. Am. A*, **21**, 169 (2004).
[31] J. Rovamo, V. Virsu, and R. Nasanen, *Nature*, **271**, 54 (1978).
[32] J. J. Koenderink, M. A. Bouman, A. E. Bueno de Mesquita, and S. Slappendale, *J. Opt. Soc. Am.*, **68**, 845 (1979).
[33] M. J. Wright and A. Johnston, *Vision Res.*, **23**, 93 (1983).
[34] A. Johnston, *J. Opt. Soc. Am. A*, **4**, 1583 (1987).
[35] D. M. Snodderly, R. S. Weinhaus, and J. C. Choi, J. Neurosci., **12**, 1169 (1992).
[36] M. D. Fairchild and G. M. Johnson, *J. Soc. Inf. Disp.*, **15**, 639 (2007).
[37] K. B. Burton, C. Owsley, and M. E. Sloane, *Vision Res.*, **33**, 939 (1993).
[38] M. J. Cox, J. H. Norma, and P. Norman, *Opthal. Physiol. Opt.*, **19**, 401 (1999).
[39] Y. J. Kim and H. S. Kim, J. Opt. Soc. Kor., **14**, 152 (2010).
[40] Y. J. Kim, *Opt. Rev.*, **17**, 459 (2010).
[41] P. G. J. Barten (SID Digest, 1991).

[42] Q. Sun and M. D. Farichild, *J. Imag. Sci. Technol.*, **48**, 211 (2004).
[43] Y. J. Kim, M. R. Luo, P. Rhodes, S. Westland, W. Choe, S. Lee, Y. Kwak, D. Park, and C. Kim, *J. Soc. Inf. Disp.*, **15**, 691 (2007)
[44] Y. J. Kim, M. R. Luo, W. Choe, H. S. Kim, S. O. Park, Y. Baek, P. Rhodes, S. Lee, and C. Kim, *J. Opt. Soc. Am. A*, **25**, 2215 (2008).
[45] R. Gong, H. Xu, B. Wang, and M. R. Luo, *Opt. Eng.*, **51**, 084001 (2013).
[46] K. Choi and H. Suk, *Opt. Eng.*, **53**, 061708 (2014).

저 자 약 력

Youn Jin Kim

• Samsung Electronic Co. Ltd. (08~Present)
• PhD in Color Science at Univ of Leeds (04~08)
• Research Interests:
Digital Color Image and Signal Processing
Mobile Computational Photography
Display Signal Processing